




Effect of the search space dimensionality for finding close and faraway targets in random searchesJ. R. Colaço ¹, H. A. Araújo,^{1,2} M. G. E. da Luz,³ G. M. Viswanathan ⁴, F. Bartumeus,^{5,6,7} and E. P. Raposo ¹¹*Laboratório de Física Teórica e Computacional, Departamento de Física, Universidade Federal de Pernambuco, Recife-PE, 50670-901, Brazil*²*Departamento de Matemática, Universidade Federal de Pernambuco, Recife-PE, 50670-901, Brazil*³*Departamento de Física, Universidade Federal do Paraná, Curitiba-PR, 81531-980, Brazil*⁴*Department of Physics and National Institute of Science and Technology of Complex Systems, Federal University of Rio Grande do Norte, Natal-RN, 59078-970, Brazil*⁵*Centre d'Estudis Avançats de Blanes-CEAB-CSIC, Girona, 17300, Spain*⁶*CREAF, Universitat Autònoma de Barcelona, Cerdanyola del Vallés, 08193, Spain*⁷*Institució Catalana de Recerca i Estudis Avançats-ICREA, Barcelona, 08010, Spain*

(Received 10 June 2022; accepted 1 September 2022; published 15 September 2022)

We investigate the dependence on the search space dimension of statistical properties of random searches with Lévy α -stable and power-law distributions of step lengths. We find that the probabilities to return to the last target found (P_0) and to encounter faraway targets (P_L), as well as the associated Shannon entropy S , behave as a function of α quite differently in one (1D) and two (2D) dimensions, a somewhat surprising result not reported until now. While in 1D one always has $P_0 \geq P_L$, an interesting crossover takes place in 2D that separates the search regimes with $P_0 > P_L$ for higher α and $P_0 < P_L$ for lower α , depending on the initial distance to the last target found. We also obtain in 2D a maximum in the entropy S for $\alpha \in (0, 2]$, not observed in 1D apart from the trivial $\alpha \rightarrow 0$ ballistic limit. Improving the understanding of the role of dimensionality in random searches is relevant in diverse contexts, as in the problem of encounter rates in biology and ecology.

DOI: [10.1103/PhysRevE.106.034124](https://doi.org/10.1103/PhysRevE.106.034124)**I. INTRODUCTION**

Random searches are important in many different contexts, from proteins seeking DNA sites to information technology and animal foraging, to name a few [1–6]. The wide range of applicability of random search processes results in part from the quite common need, even in practical everyday situations, to look for target sites whose locations are not entirely known to the searcher.

The statistical properties of random searches have been extensively investigated in the past decades [1–6]. By generally regarding the searcher as a random walker or random flier that diffuses over the search space while looking for targets, a great variety of random search models [7–38] have benefited from ideas and approaches from random walk theory, many of them primarily concerned with the animal foraging problem [1,2,39–42], in which the locations of the resource sites are unknown and the encounter rates play a significant role. In general, search models comprise as key elements the search space dimensionality, targets distribution, and the searcher's probability density functions (PDFs) of turning angles and step lengths.

One of the central statistical quantities in the random search problem is the efficiency $\eta(x_0)$ of a random search walk starting at a distance x_0 from the last target found, defined [1,2] as the number of targets located during the search path divided by the total distance traversed. In Ref. [7] the search efficiency η was first investigated both numerically

and analytically in a search model with power-law tailed PDF of step lengths, $p(\ell) \sim 1/\ell^{\alpha+1}$. This choice for $p(\ell)$ was motivated by the fact that the search dynamics is diffusive (Brownian-like) for $\alpha \geq 2$ but displays superdiffusive (Lévy-like) properties for $0 < \alpha < 2$. Indeed, superdiffusivity driven by Lévy statistics has shown to be key to the understanding of several systems, from random lasers [43–45] to particle kinetics [4,46]. According to the generalized central limit theorem (GCLT) [47,48], the family of Lévy α -stable distributions with stability index $\alpha \in (0, 2]$ is the statistical attractor of the asymptotic sum of independent and identically distributed random variables drawn from the power-law PDF of exponent $\alpha + 1$, for $0 < \alpha < 2$, with the borderline value $\alpha = 2$ converging to the Gaussian distribution driven by the CLT.

An early heuristic argument [1,7] suggested that the statistical behavior of the optimal efficiency η with respect to the Lévy index α for fixed density of targets should not depend strongly on the dimensionality of the search space. Conceivably, if the random search model defines each step as rectilinear irrespective of the landscape dimension, then the two-dimensional (2D) search path can be in principle built as a concatenation of 1D segments delimited by turning points. As shown, e.g., in Refs. [7–12], in both 1D and 2D low-density regimes the efficiency η as a function of α displays a maximum around $\alpha = 1$ for searches starting quite close to the last visited target (small x_0) and in the ballistic limit $\alpha \rightarrow 0$ when targets are initially very distant to the searcher (large

x_0). Conversely, the dependence of η on the targets density changes with dimension [12–14], as also does the average number of steps between consecutive target encounters [12].

Nevertheless, apart from the search efficiency, a systematic study addressing the dependence on the landscape dimensionality of other quantities relevant to random searches still lacks. In this work, we show that the probabilities of the searcher to return to the last target found (P_0) and to encounter faraway targets (P_L) behave quite differently in 1D and 2D, a somewhat surprising result that, to our knowledge, has not been foreseen so far. Here we obtain that, while in 1D one always has $P_0 \geq P_L$ for any x_0 and α , an interesting crossover takes place in 2D that distinguishes the search regime with $P_0 > P_L$ for higher α from the one with $P_0 < P_L$ for lower α , depending on the initial distance x_0 to the last target found.

To further characterize such differences, we investigate the Shannon entropy associated with the probabilities $P_0(x_0)$ and $P_L(x_0)$,

$$S(x_0) = -P_0 \log_2 P_0 - P_L \log_2 P_L, \quad (1)$$

with $P_0 + P_L = 1$ for any x_0 and α . We find that this function is maximized in a 2D landscape for x_0 -dependent values of α in the interval $0 < \alpha \leq 2$. In contrast, no maximum S is seen in 1D, apart from the trivial $\alpha \rightarrow 0$ ballistic limit.

This work is organized as follows. In Sec. II we set the details of the random search model and present the results for the search efficiency η , probabilities P_0 and P_L , and Shannon entropy S with Lévy and power-law PDFs of step lengths in 1D and 2D search landscapes. Whenever possible, we compare numerical results with exact analytical expressions, as in the case of P_0 , P_L , and S in 1D, with nice agreement. The relevant effect of the dimensionality of the search space on these quantities is discussed. Last, conclusions and final remarks are left to Sec. III.

II. THE MODEL: RESULTS AND DISCUSSION

We begin by setting the search landscape in 1D and 2D. Assuming that the searcher cannot jump over a target without detection, it is sufficient to define in 1D a finite search interval of length L , with target sites at the border positions $x = 0$ and $x = L$, see Fig. 1(a). A relevant quantity is the initial distance x_0 to the last target found. Due to the 1D left-right symmetry, here we choose $x_0 \leq L/2$ without loss of generality. This means that in 1D we define x_0 as the distance to the closest target (the left one at $x = 0$) at the search start (except in the fully symmetric case, $x_0 = L/2$, when both targets are initially equidistant from the searcher).

We set d as the searcher’s detection distance, so that a target is spotted when the searcher is at a distance d from it. In 1D this implies a search that effectively takes place while the searcher’s position lies in the interval $d < x < L - d$. Since the searcher cannot jump over a target, it is clear that d plays no significant role in 1D other than redefining the search spatial range, and so here we fix $d = 0$ for 1D random searches in a finite interval (in 2D, however, the searcher’s detection distance d is in fact a key quantity, see below).

For random searches in 2D, an $L \times L$ arena is set with periodic boundary conditions, see Fig. 1(b). In this case N

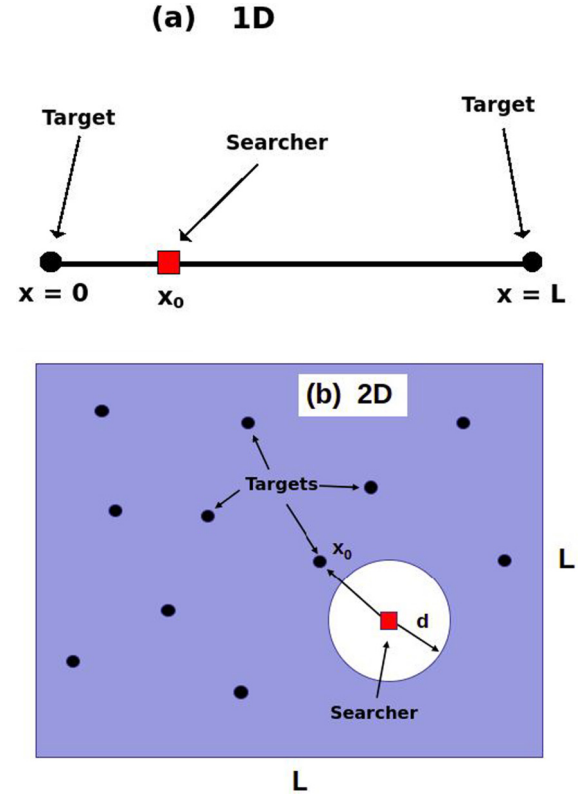


FIG. 1. Schematic random searches in 1D and 2D. (a) In 1D the searcher starts at a distance $x_0 \leq L/2$ from the closest (last visited) target in a finite interval of length L and keeps looking for a target with step lengths drawn from a probability distribution $p(\ell)$ until finding either boundary sites at $x = 0$ or $x = L$. (b) The searcher sweeps a circle of radius d (detection distance) around it along each search step in a 2D landscape of area $L \times L$, with randomly distributed targets and periodic boundary conditions.

target sites are randomly (uniformly) distributed in the 2D landscape, with targets density N/L^2 .

As for the search dynamics, we consider both in 1D and 2D that the searcher takes steps of length $\ell > 0$ from a PDF $p(\ell)$. We analyze below results for power-law and Lévy α -stable $p(\ell)$ distributions, since these PDFs have long figured as efficient choices for 1D and 2D random searches [1,2]. Regarding the step direction, we assume in 1D that steps to the right and to the left are equiprobable, whereas in 2D the step direction is drawn from a uniform angle distribution in the range $[0, 2\pi)$.

During the search process, the searcher sweeps a distance d around it along each step. If a target is detected, then the step is truncated and the search resumes with the searcher restarting at a distance $x_0 > d$ from the last visited target. Here we are interested in the low-density regime of target sites ($L \gg d$ in 1D and $N/L^2 \ll 1/d^2$ in 2D), in which it is likely that a step ends up without finding a target.

We focus on the calculation of the search efficiency η , probability P_0 of re-encountering the last target found (and its complementary probability $P_L = 1 - P_0$), and Shannon entropy associated with P_0 and P_L , Eq. (1), as functions of α and x_0 for fixed density of targets. Most results are obtained from Monte Carlo simulations with averages over 10^5 search walks

(up to 10^6 in some runs). Additionally, in 1D we also provide comparisons with results from the integral operator method [49,50],

$$\eta^{-1}(x_0) = [(\mathbb{I} - \mathcal{L})^{-1}\langle|\ell|\rangle](x_0), \quad (2)$$

$$P_L(x_0) = [(\mathbb{I} - \mathcal{L})^{-1}p_L](x_0), \quad (3)$$

where the integral operator \mathcal{L} is defined as $[\mathcal{L}f(x)'](x) = \int_0^L p(x-x')f(x')dx'$, with the kernel given by the PDF of step lengths $p(\ell)$, \mathbb{I} as the identity operator, and $\langle|\ell|\rangle(x_0)$ and $p_L(x_0)$ denoting, respectively, the mean step length to find a target in 1D and the probability of encountering the target at $x = L$ in a single step starting from $x = x_0$. For the mean step length, we explicitly write

$$\begin{aligned} \langle|\ell|\rangle(x_0) = & \int_{-x_0}^0 |\ell|p(\ell)d\ell + \int_0^{L-x_0} \ell p(\ell) \\ & + x_0 \int_{-\infty}^{-x_0} p(\ell)d\ell + (L-x_0) \int_{L-x_0}^{\infty} p(\ell)d\ell, \end{aligned} \quad (4)$$

where in the first (last) two integrals a boundary target is not (is) found. Since for power law and Lévy $p(\ell)$ the inverse operator $(\mathbb{I} - \mathcal{L})^{-1}$ in Eqs. (2) and (3) is not known analytically in continuous space, then we express it in matrix form on discretization [51] of the 1D search interval through $x = j\Delta x$, with integer j and $\Delta x/L \ll 1$ (here we set $\Delta x/L = 2 \times 10^{-4}$).

In 1D our results are also compared with exact analytical expressions for P_0 , P_L , and S . To our knowledge, so far no exact analytical results for such quantities are available in 2D.

A. Power-law distribution

We consider initially the power-law (Pareto) PDF of step lengths in the form

$$p(\ell) = \frac{\alpha \ell_0^\alpha}{\ell^{\alpha+1}}, \quad \ell \geq \ell_0, \quad (5)$$

and $p(\ell) = 0$ otherwise, where ℓ_0 sets the minimum step length and the parameter $\alpha > 0$ controls the tail shape and fluctuations magnitude ($\alpha \leq 0$ does not yield a normalizable distribution). Indeed, for $\alpha > 2$ the variance of the PDF (5) is finite, so that the sum of a large number of independent power-law random variables displays Gaussian statistics driven by the CLT. Conversely, in the heavy-tailed case with $0 < \alpha < 2$ the diverging variance implies much stronger fluctuations and Lévy statistics of the variables sum governed by the GCLT (the borderline case $\alpha = 2$ is also driven by the CLT) [47,48]. So, by varying only the single parameter α , both diffusive Gaussian-like and superdiffusive Lévy-like search dynamics can be accessed with the power-law PDF of step lengths. The minimum step length ℓ_0 is in principle a free parameter to choose. However, in the present search context a preferable choice in numerical simulations should be ℓ_0 not larger than the initial distance x_0 to the closest target. We also remark that Eq. (5) with a proper expression [47,48] for ℓ_0 and $0 < \alpha < 2$ represents the large- ℓ limit of the Lévy α -stable distribution (see next subsection).

I. Results for 1D landscape

We start with the discussion of the 1D results. Figure 2(a) presents the search efficiency η as a function of α . A nice agreement is noticed between the Monte Carlo (circles) and integral operator [squares, Eq. (2)] results for $L = 10^3$ (targets density $L^{-1} = 10^{-3}$), $\ell_0 = 0.2$, $d = 0$, and several values of x_0 [lines in Fig. 2(a) are a guide to the eye]. In particular, the so-called asymmetric nondestructive and symmetric destructive regimes [1,2] correspond, respectively, to the searcher starting very close to the last target found ($x_0/L \ll 1$) and very far from it ($x_0/L = 1/2$). In the latter, the maximum efficiency is achieved in the large-step ballistic limit $\alpha \rightarrow 0$, which favors the encounter of faraway targets in just one single step. Indeed, for $x_0/L = 1/2$ we obtain the maximum efficiency $\eta_{\max} \rightarrow 1/x_0 = 0.002$ when $\alpha \rightarrow 0$, in agreement with Fig. 2(a) (black symbols).

On the other hand, in the asymmetric nondestructive regime with $x_0/L \ll 1$ a compromise balance between large ($\alpha \rightarrow 0$) and small ($\alpha \geq 2$) steps to find, respectively, far and nearby targets leads to a maximum efficiency for $\alpha \approx 1$, as depicted in blue symbols in Fig. 2(a) for $x_0 = 0.4$. Figure 2(a) also shows for intermediate x_0/L that the efficiency is maximized at values $\alpha = \bar{\alpha}(x_0)$ that decrease with x_0 and are restricted to the interval $0 < \bar{\alpha}(x_0) \leq 1$. These findings on the search efficiency η have been reported in the literature [1,2].

We next turn to investigate the probability P_0 of finding the last visited target after starting at a distance x_0 from it and the complementary probability P_L (in 1D P_L concerns the encounter of the target at the initial distance $L - x_0$ from the searcher). Figure 2(b) displays a nice agreement between the Monte Carlo results (circles) and exact analytical expressions [49,50] for P_0 and P_L (solid lines), where

$$P_L(x_0, \alpha) = f(x_0, \alpha) \left(\frac{x_0}{L}\right)^{\alpha/2}, \quad (6)$$

for $\ell_0 \rightarrow 0$, with

$$f(x_0, \alpha) = \frac{2 {}_2F_1(\alpha/2, 1 - \alpha/2; 1 + \alpha/2; x_0/L)}{\alpha B(\alpha/2, \alpha/2)}, \quad (7)$$

in which ${}_2F_1$ and B denote, respectively, hypergeometric and beta functions. As noticed in Fig. 2(b), these results also compare nicely with those obtained from the integral operator method [squares, Eq. (3)].

When the searcher starts symmetrically from the middle of the 1D interval, $x_0/L = 1/2$, Fig. 2(b) shows in black symbols that the finding of any of the two boundary targets is equiprobable, i.e., $P_0 = P_L = 1/2$ for any α , as expected. However, as x_0 decreases, that is, as the searcher begins closer to the last visited target, P_0 increases monotonically for any given value of α . We also observe in Fig. 2(b) that $P_0 > P_L$ for all $x_0/L < 1/2$ and $\alpha > 0$. This indicates that in 1D the last target found is *always* encountered with *higher* probability if compared to the finding of the faraway target. As we shall see below, this result does not hold in 2D, and an interesting crossover regarding the probabilities P_0 and P_L emerges as a function of x_0 and α in 2D random searches.

The 1D results for P_0 and P_L in Fig. 2(b) can be also read off from Fig. 2(c) in terms of the Shannon entropy S , Eq. (1). A nice agreement between exact (solid lines), Monte Carlo (circles), and integral operator method (squares) results

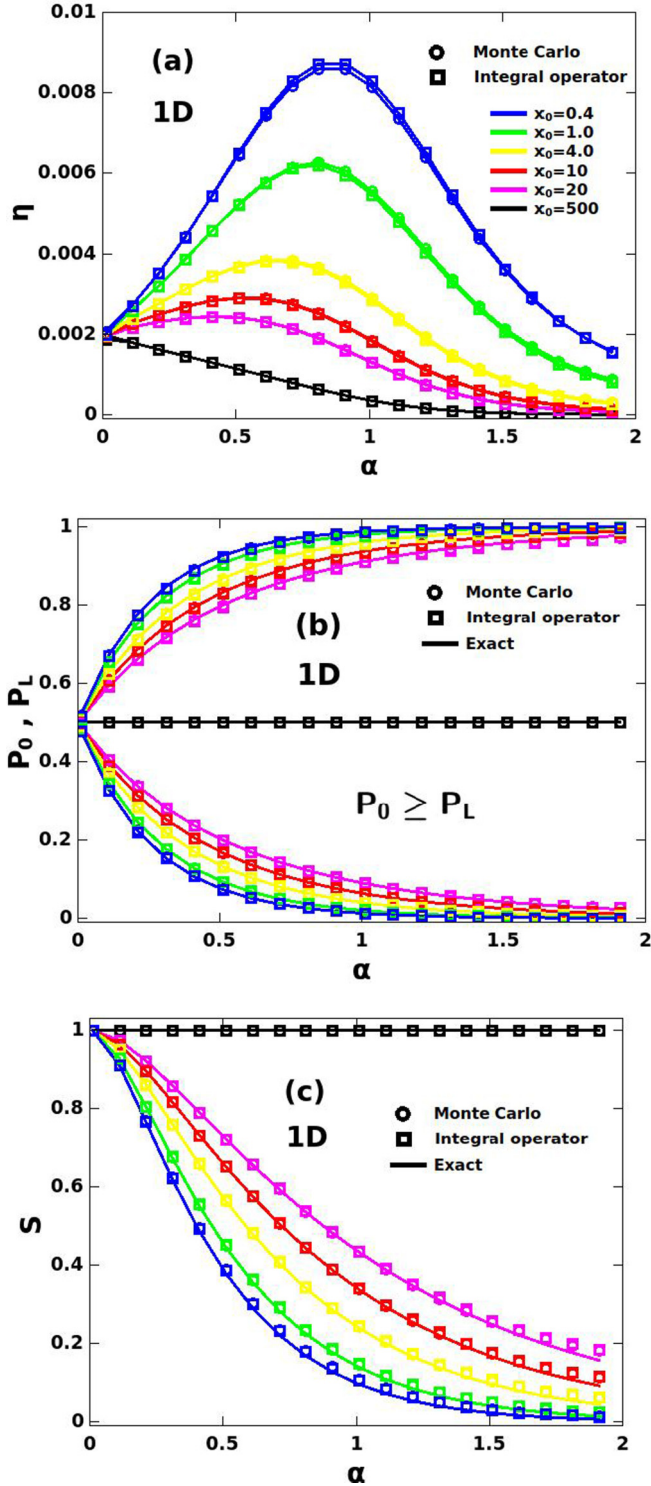


FIG. 2. One-dimensional random searches. (a) Efficiency η , (b) probabilities to find the closest (P_0) and distant (P_L) targets, and (c) associated Shannon entropy S as a function of the exponent α of the power law $p(\ell)$, Eq. (5), for $L = 10^3$, $\ell_0 = 0.2$, $d = 0$, and various x_0 [colors in (b) and (c) are the same as in (a)]. Monte Carlo and integral operator [Eqs. (2) and (3)] results are shown in circles and squares, respectively. Solid lines depict exact results [Eqs. (6) and (7)] in (b) and (c) and are a guide to the eye in (a). P_0 (P_L) in (b) corresponds to the curves above (below) the line $P_0 = P_L = 1/2$, since $P_0 \geq P_L$ for any x_0 and α in 1D. Nice agreement is noticed between Monte Carlo, integral operator, and exact results.

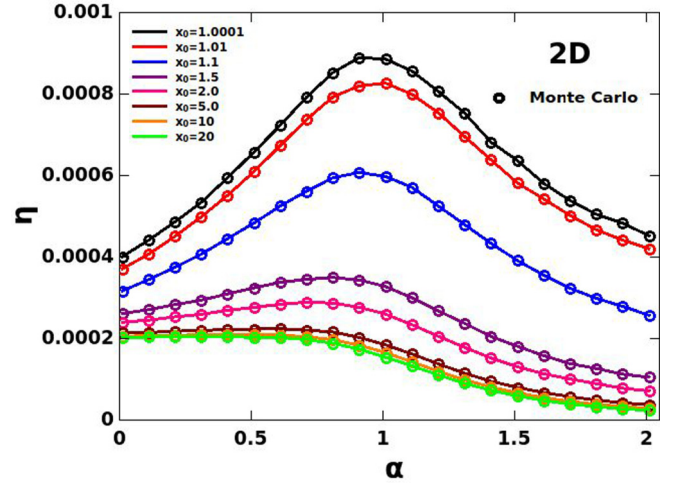


FIG. 3. Two-dimensional random searches. Efficiency η as a function of the exponent α of the power law $p(\ell)$ for 10^6 randomly distributed targets, $L \times L = 10^{10}$, $\ell_0 = 0.1$, $d = 1$, and various x_0 . Monte Carlo results are shown in symbols and solid lines are a guide to the eye. As in 1D searches, the maximum η is achieved for $\alpha \approx 1$ when $x_0 \rightarrow d$. Notice also the plateau in η for $\alpha \lesssim 0.5$ and $x_0 \gtrsim 5$, which is not seen in 1D searches [compare with Fig. 2(a)].

for S is seen in Fig. 2(c). The equiprobability to find either targets when $x_0/L = 1/2$ (fully symmetric regime) is depicted in Fig. 2(c) by the maximum value $S = 1$ observed for all α (black symbols). Also, the 1D monotonic behavior of P_0 and P_L as functions of x_0 and α implies that S always decreases with α for fixed x_0 , and always increases with x_0 for fixed α . To understand this behavior, we first observe that the large-step ballistic limit $\alpha \rightarrow 0$ makes both boundary targets to be likely found in the very first step, irrespective of the searcher's starting distance x_0 . In this case, since steps to the right and to the left are equiprobable in 1D, we notice that $P_0 = P_L = 1/2$, leading to the maximum entropy value $S = 1$ in Fig. 2(c) for any x_0 and $\alpha \rightarrow 0$.

On the other hand, the maximum entropy $S = 1$ is *not* observed in Fig. 2(c) for $x_0/L < 1/2$ and $\alpha > 0$, consistent with the fact that, apart from the 1D fully symmetric regime, P_0 is always greater than P_L . The difference between P_0 and P_L becomes monotonically larger, and so S decreases monotonically, either when the searcher starts closer to the last visited target (smaller x_0) or when the probability of large steps is lower (higher α). The absence of a maximum in S for $\alpha > 0$ in 1D random searches notably contrasts with the quite distinct S behavior in 2D searches discussed below.

2. Results for 2D landscape

We now study random searches in a 2D landscape with power-law distribution $p(\ell)$. Monte Carlo simulations were performed with $N = 10^6$ targets, $L = 10^5$ (targets density $N/L^2 = 10^{-4}$), $\ell_0 = 0.1$, $d = 1$, and several values of x_0 .

We first notice in Fig. 3 that the search efficiency η in 2D behaves as a function of α and x_0 in a way similar to the 1D case [compare with Fig. 2(a)]. This includes both nondestructive ($x_0/L \ll 1$) and destructive ($x_0/L \sim 1/2$) regimes, in which the maximum efficiency for low targets density

is achieved as in 1D for $\alpha \approx 1$ and $\alpha \rightarrow 0$, respectively. Nevertheless, it is also worth noticing that a sort of plateau establishes [9] in η for $\alpha \lesssim 0.5$ and $x_0 \gtrsim 5$, indicating that, differently from 1D searches, no significant gain in the 2D search efficiency takes place over this range of parameters. Moreover, as well as in 1D, we observe for intermediate x_0/L in 2D that the value $\alpha = \bar{\alpha}(x_0) \in (0, 1]$ at which η is maximum generally decreases with x_0 .

However, a remarkable change in the probabilities P_0 and P_L and Shannon entropy S can be observed in 2D searches in Figs. 4 and 5, respectively. For $x_0 \gtrsim 1.01$ a crossover not reported so far takes place in P_0 and P_L in 2D, which is not present in 1D [compare Figs. 2(b) and 4]. This crossover separates the 2D search regime with $P_0 < P_L$ for lower α from the one with $P_0 > P_L$ for higher α (recall that $P_0 \geq P_L$ for any x_0 and α in 1D). For instance, we note in Fig. 4(a) that when $x_0 = 1.1$ (blue symbols) $P_0 < P_L$ for $\alpha \lesssim 0.3$. This range widens for larger x_0 values [e.g., $P_0 < P_L$ for $\alpha \lesssim 1.8$ when $x_0 = 5$, brown symbols in Fig. 4(c)].

The 2D crossover in P_0 and P_L also manifests itself in the Shannon entropy through the emergence of a maximum $S = 1$ at values $\alpha > 0$, which is not seen for non-null α in 1D [compare Figs. 2(c) and 5]. This maximum takes place at the α value for which $P_0 = P_L = 1/2$. Consistent with Fig. 4, the maximum S occurs at higher α values for larger x_0 .

The physical origin of this crossover lies in the fact that in 2D the searcher can actually pass very close to a target (at a distance $\gtrsim d$) without detecting it. Take, for instance, the very first step of a searcher starting at a small distance $x_0 \gtrsim d$ from the last visited target. If in 2D the searcher does not take the step direction within the correct angle range, then it will miss the detection circle of radius d around the closest target and, in the large- ℓ limit of small α , will be likely head to a great distance from the starting point already in the first step. (Note that the probability of missing the closest target in 2D tends to one as the searcher's detection distance $d \rightarrow 0$; this highlights the relevance of the parameter d in 2D, in contrast with the 1D case.)

It is thus clear that, depending on the values of x_0 and α , the probability of finding the last visited target in a 2D search path can be actually lower than the one of encountering any other target, $P_0 < P_L$. A maximum S then arises in 2D when $P_0 = P_L$ for specific values of x_0 and $\alpha > 0$.

This reasoning clearly does not apply in 1D, since in this case the searcher cannot miss a target by jumping over it without detection. Thus, in 1D one always ends up with $P_0 \geq P_L$ for any $x_0 \leq L/2$ and α , as discussed, with the maximum entropy S achieved only in the ballistic limit $\alpha \rightarrow 0$.

B. Lévy distribution

A random variable $u \in (-\infty, \infty)$ is distributed according to the family of Lévy α -stable distributions if its PDF is given by [47,48]

$$p(u) = \frac{1}{2\pi} \int_{-\infty}^{\infty} dk e^{-|ck|^{\alpha}[1-\beta\text{sgn}(k)\Phi(k)]-ik(u-v)}. \quad (8)$$

The Lévy stability index $\alpha \in (0, 2]$ is the most important parameter since it drives the main statistical properties of u .

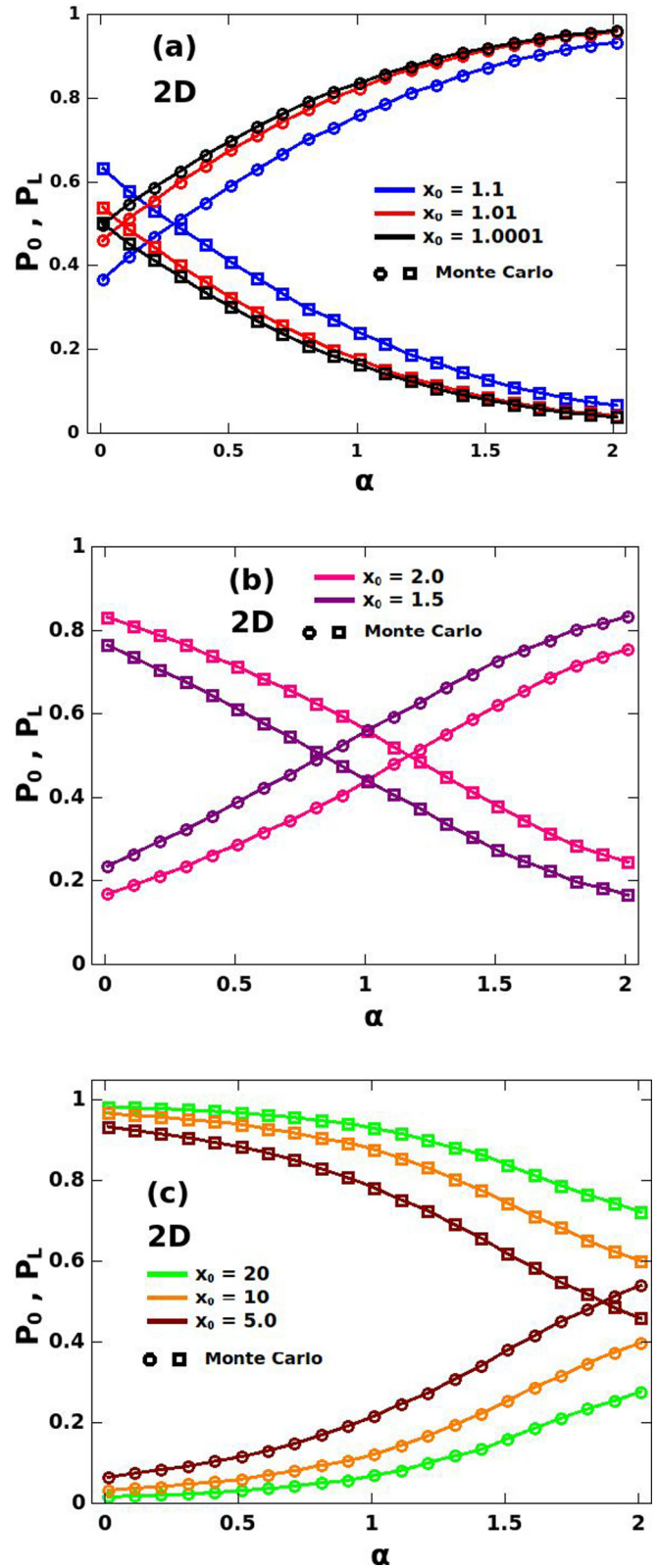


FIG. 4. Two-dimensional random searches. Probabilities to find the closest (P_0) and distant (P_L) targets as a function of the exponent α of the power law $p(\ell)$. Monte Carlo results are shown in symbols and solid lines are a guide to the eye (parameters as in Fig. 3). P_0 and P_L depicted by circles and squares, respectively, display an interesting crossover not present in 1D [compare with Fig. 2(b)].

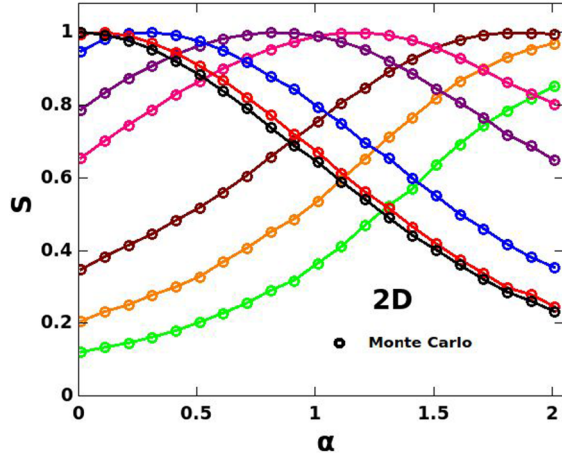


FIG. 5. Two-dimensional random searches. Shannon entropy S as a function of the exponent α of the power law $p(\ell)$. Monte Carlo results are shown in symbols and solid lines are a guide to the eye (parameters and colors as in Figs. 3 and 4). The maxima in S , not observed in 1D apart from trivial $\alpha \rightarrow 0$ ballistic limit, take place at the α value where $P_0 = P_L = 1/2$ for each x_0 in Fig. 4.

Indeed, whereas the borderline value $\alpha = 2$ corresponds to the Gaussian distribution governed by the CLT, the GCLT sets the fluctuation dynamics of the variable u when $0 < \alpha < 2$. In addition, $\beta \in [-1, 1]$ is the asymmetry (skewness) parameter, $c > 0$ is a scale factor, v is a shift (location) parameter, sgn is the sign function, and $\Phi = \tan(\pi\alpha/2)$ if $\alpha \neq 1$ and $\Phi(k) = (-2/\pi) \log |k|$ if $\alpha = 1$. For nonskewed distributions centered at $u = 0$, one sets $\beta = 0$ and $v = 0$ in Eq. (8). In this work, with positive-defined step lengths, we consider Lévy PDFs $p(\ell) = p(|u|) + p(-|u|) = 2p(|u|)$, in the $\ell > 0$ domain.

We remark as well that, by expanding the Lévy $p(\ell)$ in Taylor series in the large- ℓ limit for $0 < \alpha < 2$, one obtains [47,48] the power-law PDF (5), but with $\alpha\ell_0^\alpha$ replaced by $2c^\alpha\Gamma(\alpha + 1)\sin(\pi\alpha/2)/\pi$.

The fact that the power-law PDF actually represents the large- ℓ limit of the Lévy distribution for $0 < \alpha < 2$ renders the results of the efficiency η , probabilities P_0 and P_L , and Shannon entropy S to be qualitatively similar for these distributions of step lengths. So, in order to avoid unnecessary repetition of akin results for η , P_0 , P_L , and S as functions of α and x_0 , and to focus on previously undiscussed issues, in Fig. 6(a) we present for several x_0 the value $\alpha = \alpha^*$ at which the Shannon entropy has the maximum $S = 1$ in 2D, for both Lévy (black circles) and power-law (red squares) PDFs. In particular, we mention that our 2D Monte Carlo results for the Lévy $p(\ell)$ were obtained using McCulloch’s algorithm for sampling Lévy distributed random numbers [52], with $N = 10^6$, $L = 10^5$ (targets density $N/L^2 = 10^{-4}$), $c = 1$, $d = 1$, and various x_0 .

By comparing Fig. 3 and Fig. 6(a) we notice that the values of α that maximize the Shannon entropy S in 2D for each x_0 and fixed targets density do not coincide with those at which the 2D search efficiency η is maximum with the same parameters. Indeed, while we observe in Fig. 3 that the $\bar{\alpha}$ values of maximum η decrease for larger x_0 and are restricted

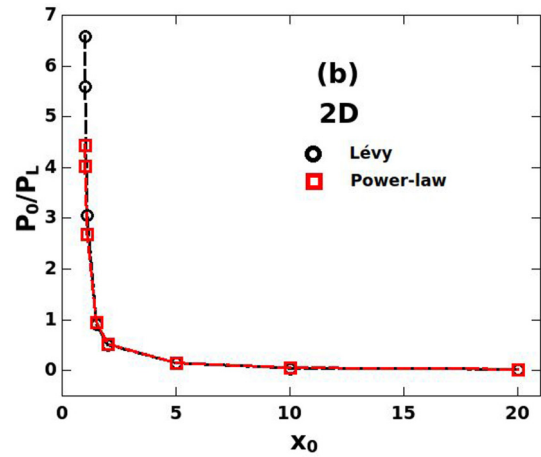
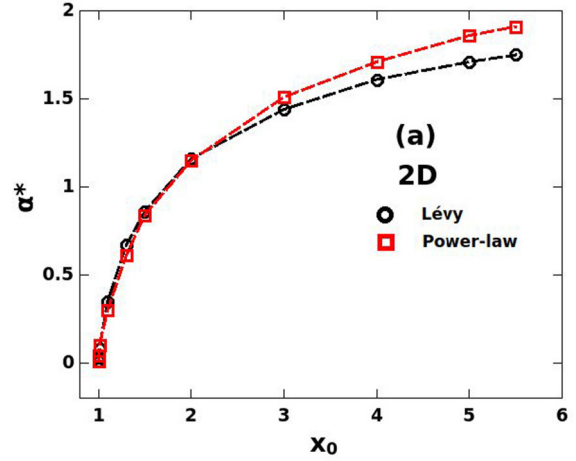


FIG. 6. Two-dimensional random searches. (a) Loci of the points of maximum in the Shannon entropy S . The maxima S take place at the value $\alpha = \alpha^*$ where $P_0 = P_L = 1/2$ for each x_0 , with the other parameters as in Figs. 3–5. Black circles and red squares depict, respectively, results with Lévy and power-law distributions $p(\ell)$ of step lengths. Dashed lines are best fits to the logarithmic growth of α^* with x_0 , Eq. (9). (b) Ratio P_0/P_L in which the 2D efficiency η is maximum for various x_0 . Dashed lines are a guide to the eye.

to the interval $\bar{\alpha} \in (0, 1]$, a quite opposite trend is seen in Fig. 6(a), with α^* increasing with x_0 in the broader range $\alpha^* \in (0, 2]$. Since S only regards the probabilities of finding targets, and does not account for the traversed distances relevant to determine η , then it is actually conceivable that the mentioned mechanism of compromise balance that leads to the maximum η does not correspond to the one discussed above for the maximization of S .

We further observe in Fig. 6(a) that the curves for the Lévy and power-law PDFs nearly coincide for $0 < \alpha \lesssim 1$, since this range favors larger ℓ values corresponding to the Taylor expansion of the Lévy distribution in power-law form. On the other hand, in the interval $1 \lesssim \alpha < 2$ the maximum S for a given x_0 is obtained with a slightly higher α in the power law $p(\ell)$. In fact, as the borderline value $\alpha = 2$ of Gaussian-like dynamics approaches, small steps with $\ell < \ell_0$ are forbidden in the power-law PDF, Eq. (5), but not in the Lévy distribution. In this case, and for x_0 not too small

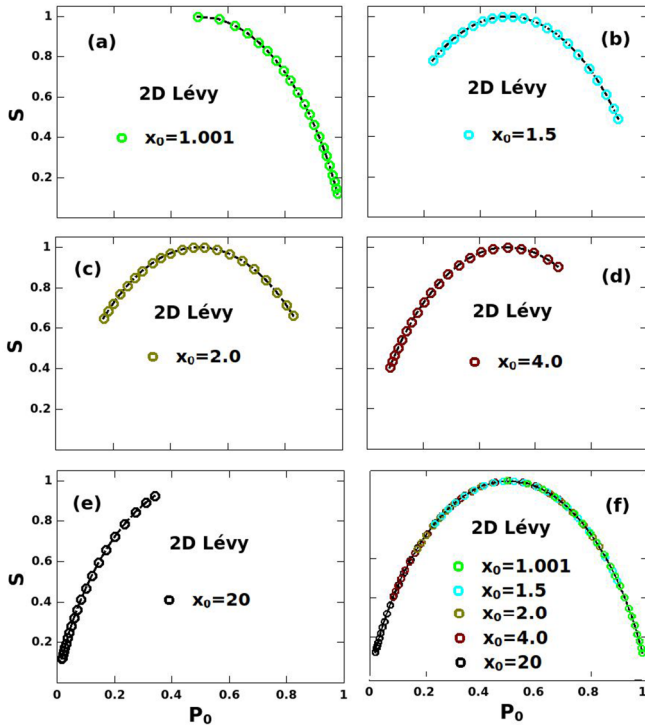


FIG. 7. Two-dimensional random searches. Shannon entropy S versus probability P_0 to find the last visited target with Lévy PDF of step lengths. Each point in (a)–(e) corresponds to specific values of x_0 and α . Solid lines are a guide to the eye. The superposition of the curves in (a)–(e) is displayed in (f), with the standard profile of the Shannon entropy. Results of 1D random searches for any x_0 are similar to those in (a). The S behavior in (b)–(e) is not found in 1D random searches.

[e.g., $x_0 \approx 5$ in Fig. 6(a)], the condition $P_0 = P_L = 1/2$ for the maximum $S = 1$ is fulfilled for a little higher α in the power law $p(\ell)$.

Regarding the form of the curves in Fig. 6(a), we first remark that P_0 , P_L , and S should in fact be functions of the dimensionless reduced variable $\bar{x}_0 = (x_0 - d)/L$, with $x_0 - d$ expressing the effective initial distance to the last visited target in 2D. The ballistic limit $\alpha^* \rightarrow 0$ in Fig. 6(a) corresponds to $x_0 \rightarrow d$ (or $\bar{x}_0 \rightarrow 0$), indicating in this case that the findings of the initially very close and faraway targets occur with same probability in the 2D landscape, see also Fig. 5. In the regime with $\bar{x}_0 \rightarrow 0$ the motion of the random searcher near the border of the detection circle of radius d around the closest target is essentially one dimensional, and so one expects [12] the 1D scaling form $P_L \sim \bar{x}_0^{\alpha/2}$ still to hold, see Eq. (6). By differentiating S with respect to α in the limit $\alpha \rightarrow 0$, we find $\alpha^* \sim \ln(1 + \gamma \bar{x}_0)$, with some constant γ so to concur with the ballistic limit $\alpha^* \rightarrow 0$ as $\bar{x}_0 \rightarrow 0$ for fixed $L \gg x_0$. Actually, even for α^* not too close to zero a nice fit to the logarithmic growth of α^* with x_0 is observed for both PDFs in Fig. 6,

$$\alpha^* = \frac{1}{b} \ln[1 + (x_0 - d)/a], \quad (9)$$

with best fit values $a = 0.13$ and $b = 1.88$ for the power law $p(\ell)$ and $a = 0.06$ and $b = 2.50$ for the Lévy, consistent with the faster increase of the latter.

A complementary view of these findings can be seen in Fig. 6(b), with the plot of the ratio P_0/P_L in which the efficiency η is maximum for various x_0 . With both Lévy and power-law PDFs, we notice that the values of P_0/P_L that optimize η vary over a broad range and are generally different from $P_0/P_L = 1$, the ratio at which S is maximum.

Finally, we investigate in Fig. 7 the behavior of the Shannon entropy S with the probability P_0 for several values of x_0 in 2D Lévy searches. Each point in Figs. 7(a)–7(e) corresponds to specific values of x_0 and α . We start by noticing for a quite small $x_0 = 1.001$ in Fig. 7(a) that S is fully asymmetric regarding $P_0 = 1/2$, with the maximum $S = 1$ occurring at $P_0 = 1/2$ for $\alpha \rightarrow 0$ ballistic searches, as discussed. For $x_0 = 1.001$ and larger α the probability P_L to reach faraway targets gets lower, and so the probability P_0 to re-encounter the closest target increases, $P_0 > 1/2$ in Fig. 7(a), causing S to decrease. As x_0 grows, the asymmetry regarding $P_0 = 1/2$ reduces and one actually finds $P_0 < 1/2$ (i.e., $P_0 < P_L$) for a range of α , see Fig. 7(b) and Fig. 7(c) for $x_0 = 1.5$ and $x_0 = 2$, respectively. Progressively larger x_0 values invert the trend of Fig. 7(a), yielding $P_0 < P_L$ for most α , as shown in Fig. 7(d) for $x_0 = 4$. Last, for large-enough x_0 , e.g., $x_0 = 20$ in Fig. 7(e), we obtain $P_0 < P_L$ for any $\alpha \in (0, 2]$ in 2D Lévy searches. Figure 7(f) presents the superposition of the curves of S for the various x_0 , Figs. 7(a)–7(e), displaying the standard profile of the Shannon entropy.

Regarding the comparison with 1D searches, since in this case $P_0 \geq P_L$ (i.e., $P_0 \geq 1/2$) for any x_0 and α , then S as a function of P_0 in 1D is qualitatively similar to Fig. 7(a). Actually, the 2D results of Figs. 7(b)–7(e) do not have a counterpart in 1D random searches.

III. CONCLUSIONS

In conclusion, in this work we have investigated the effect of the landscape dimensionality on a number of quantities statistically relevant to random searches. By considering Lévy α -stable and power-law distributions of step lengths, we have obtained that the probabilities to return to the last target found and to encounter faraway targets, as well as the associated Shannon entropy, are importantly affected by the search space dimension.

The parameters space of 2D random searches in the low targets density regime was found to be bipartite, with $P_0 > P_L$ for higher α and $P_0 < P_L$ for lower α , depending on the distance x_0 to the last target found. This finding contrasts with the 1D case, in which $P_0 \geq P_L$ for any x_0 and α . Further, for each value of x_0 the associated Shannon entropy in 2D searches presents a maximum in the range $0 < \alpha \leq 2$, which does not occur in 1D landscapes. In particular, entropy is a fundamental quantity to understand landscape ecology (see, e.g., Ref. [53]), and here we have shown that dimensionality is central to the entropy behavior associated with the finding of near and faraway targets as a function of α . On the other hand, the mechanisms of search optimization cannot be explained

only in terms of an entropy solely relying on the encounter probabilities P_0 and P_L . These results thus pose the important question of what should be a suitable definition of entropy to characterize random search processes.

Random searchers have many applications in several systems in which the dimensionality of the search space is key, as in the foraging problem in biology and ecology, in which encounter rates play a major role. Thus, addressing the question of how statistically relevant quantities behave with dimension can be of paramount importance. We hope our findings can stimulate further theoretical and experimental research to advance the overall understanding of random search processes.

ACKNOWLEDGMENTS

We thank Sergey V. Buldyrev for collaboration in the early stages of this work, and for a critical reading and suggestions to this manuscript. This work was partially supported by the Brazilian agencies Conselho Nacional de Desenvolvimento Científico e Tecnológico (CNPq), Coordenação de Aperfeiçoamento de Pessoal de Nível Superior (CAPES), and Fundação de Amparo a Ciência e Tecnologia do Estado de Pernambuco (FACEPE). E.P.R., M.G.E.L., and G.M.V. acknowledge CNPq Grants No. 305062/2017-4, No. 304532/2019-3, and No. 302051/2018-0, respectively. F.B. acknowledges Spanish Ministry of Science Grant No. (GL2016-78156-C2-1-R).

-
- [1] G. M. Viswanathan, M. G. E. da Luz, E. P. Raposo, and H. E. Stanley, *The Physics of Foraging* (Cambridge University Press, Cambridge, UK, 2011).
- [2] V. Méndez, D. Campos, and F. Bartumeus, *Stochastic Foundations in Movement Ecology* (Springer, Berlin, 2014).
- [3] M. G. E. da Luz, A. Grosberg, E. P. Raposo, and G. M. Viswanathan, *J. Phys. A: Math. Theor.* **42**, 430301 (2009).
- [4] V. Zaburdaev, S. Denisov, and J. Klafter, *Rev. Mod. Phys.* **87**, 483 (2015).
- [5] A. V. Chechkin, V. Y. Gonchar, J. Klafter, and R. Metzler, *Adv. Chem. Phys.* **133**, 439 (2006).
- [6] O. Bénichou, C. Loverdo, M. Moreau, and R. Voituriez, *Rev. Mod. Phys.* **83**, 81 (2011).
- [7] G. M. Viswanathan, S. V. Buldyrev, S. Havlin, M. G. E. da Luz, E. P. Raposo, and H. E. Stanley, *Nature (Lond.)* **401**, 911 (1999).
- [8] E. P. Raposo, S. V. Buldyrev, M. G. E. da Luz, M. C. Santos, H. E. Stanley, and G. M. Viswanathan, *Phys. Rev. Lett.* **91**, 240601 (2003).
- [9] M. C. Santos, E. P. Raposo, G. M. Viswanathan, and M. G. E. da Luz, *Europhys. Lett.* **67**, 734 (2004).
- [10] F. Bartumeus and S. A. Levin, *Proc. Natl. Acad. Sci. USA* **105**, 19072 (2008).
- [11] A. M. Reynolds and F. Bartumeus, *J. Theor. Biol.* **260**, 98 (2009).
- [12] S. V. Buldyrev, E. P. Raposo, F. Bartumeus, S. Havlin, F. R. Rusch, M. G. E. da Luz, and G. M. Viswanathan, *Phys. Rev. Lett.* **126**, 048901 (2021).
- [13] N. Levernier, J. Textor, O. Bénichou, and R. Voituriez, *Phys. Rev. Lett.* **124**, 080601 (2020).
- [14] N. Levernier, J. Textor, O. Bénichou, and R. Voituriez, *Phys. Rev. Lett.* **126**, 048902 (2021).
- [15] F. Bartumeus, F. Peters, S. Pueyo, C. Marrasé, and J. Catalan, *Proc. Natl. Acad. Sci. USA* **100**, 12771 (2003).
- [16] G. Ramos-Fernández, J. L. Mateos, O. Miramontes, C. Germinal, H. Larralde, and B. Ayala-Orosco, *Behav. Ecol. Sociobiol.* **55**, 223 (2004).
- [17] O. Bénichou, M. Coppey, M. Moreau, P.-H. Suet, and R. Voituriez, *J. Phys.: Condens. Matter* **17**, S4275 (2005).
- [18] A. M. Reynolds, *Europhys. Lett.* **75**, 517 (2006).
- [19] S. Benhamou, *Ecology* **88**, 1962 (2007).
- [20] A. Reynolds, *Ecology* **89**, 2347 (2008).
- [21] D. W. Sims, E. J. Southall, N. E. Humphries, G. C. Hays, C. J. A. Bradshaw, J. W. Pitchford, A. James, M. Z. Ahmed, A. S. Brierley, M. A. Hindell, D. Morritt, M. K. Musyl, D. Righton, E. L. C. Shepard, V. J. Wearmouth, R. P. Wilson, M. J. Witt, and J. D. Metcalfe, *Nature (Lond.)* **451**, 1098 (2008).
- [22] E. A. Codling, M. J. Plank, and S. Benhamou, *J. R. Soc. Interface* **5**, 813 (2008).
- [23] A. James, M. J. Plank, and R. Brown, *Phys. Rev. E* **78**, 051128 (2008).
- [24] M. A. Lomholt, T. Koren, R. Metzler, and J. Klafter, *Proc. Natl. Acad. Sci. USA* **105**, 11055 (2008).
- [25] M. F. Shlesinger, *J. Phys. A: Math. Theor.* **42**, 434001 (2009).
- [26] L. Giuggioli, F. J. Sevilla, and V. M. Kenkre, *J. Phys. A: Math. Theor.* **42**, 434004 (2009).
- [27] D. Boyer, O. Miramontes, and H. Larralde, *J. Phys. A: Math. Theor.* **42**, 434015 (2009).
- [28] N. E. Humphries, N. Queiroz, J. R. M. Dyer, N. G. Pade, M. K. Musyl, K. M. Schaefer, D. W. Fuller, J. M. Brunnschweiler, T. K. Doyle, J. D. R. Houghton, G. C. Hays, C. S. Jones, L. R. Noble, V. J. Wearmouth, E. J. Southall, and D. W. Sims, *Nature (Lond.)* **465**, 1066 (2010).
- [29] P. Schultheiss and K. Cheng, *Anim. Behav.* **81**, 1031 (2011).
- [30] S. Petrovskii, A. Mashanova, and V. A. A. Jansen, *Proc. Natl. Acad. Sci. USA* **108**, 8704 (2011).
- [31] M. de Jager, F. J. Weissing, P. M. J. Herman, B. A. Nolet, and J. van de Koppel, *Science* **332**, 1551 (2011).
- [32] V. A. A. Jansen, A. Mashanova, and S. Petrovskii, *Science* **335**, 918 (2012).
- [33] O. Miramontes, O. DeSouza, L. R. Paiva, A. Marins, and S. Orozco, *PLoS One* **9**, e111183 (2014).
- [34] A. M. Reynolds, *Sci. Rep.* **4**, 4409 (2014).
- [35] M. E. Wosniack, M. C. Santos, E. P. Raposo, G. M. Viswanathan, and M. G. E. da Luz, *Phys. Rev. E* **91**, 052119 (2015).
- [36] L. Riotte-Lambert, S. Benhamou, and S. Chamailé-Jammes, *Behav. Ecol.* **28**, 280 (2017).
- [37] T. Dannemann, D. Boyer, and O. Miramontes, *Proc. Natl. Acad. Sci. USA* **115**, 3794 (2018).
- [38] J. Ferreira, E. P. Raposo, H. A. Araújo, M. G. E. da Luz, G. M. Viswanathan, F. Bartumeus, and D. Campos, *Phys. Rev. E* **103**, 022105 (2021).
- [39] D. W. Stephens and J. R. Krebs, *Foraging Theory* (Princeton University Press, Princeton, NJ, 1987).

- [40] H. C. Berg, *Random Walks in Biology* (Princeton University Press, Princeton, NJ, 1993).
- [41] P. Turchin, *Quantitative Analysis of Movement* (Sinauer Associates Inc., Sunderland, 1998).
- [42] A. C. Kamil and T. D. Sargent (eds.), *Foraging Behavior: Ecological, Ethological, and Psychological Approaches* (Garland STPM Press, New York, 1981).
- [43] A. S. L. Gomes, A. L. Moura, C. B. de Araújo, and E. P. Raposo, *Prog. Quant. Electron.* **78**, 100343 (2021).
- [44] E. P. Raposo and A. S. L. Gomes, *Phys. Rev. A* **91**, 043827 (2015).
- [45] B. C. Lima, P. I. R. Pincheira, E. P. Raposo, L. S. Menezes, C. B. de Araújo, A. S. L. Gomes, and R. Kashyap, *Phys. Rev. A* **96**, 013834 (2017).
- [46] B. B. Mandelbrot, *The Fractal Geometry of Nature* (Freeman, New York, 1982).
- [47] V. M. Zolotarev and V. M. Uchaikin, *Chance and Stability* (VSP BV, Utrecht, 1999).
- [48] G. Samorodnitsky and M. S. Taqqu, *Stable Non-Gaussian Random Processes* (Chapman & Hall, New York, 1994).
- [49] S. V. Buldyrev, S. Havlin, A. Y. Kazakov, M. G. E. da Luz, E. P. Raposo, H. E. Stanley, and G. M. Viswanathan, *Phys. Rev. E* **64**, 041108 (2001).
- [50] S. V. Buldyrev, M. Gitterman, S. Havlin, A. Y. Kazakov, M. G. E. da Luz, E. P. Raposo, H. E. Stanley, and G. M. Viswanathan, *Physica A* **302**, 148 (2001).
- [51] F. Bartumeus, E. P. Raposo, G. M. Viswanathan, and M. G. E. da Luz, *PLoS One* **9**, e106373 (2014).
- [52] J. M. Chambers, C. L. Mallows, and B. W. Stuck, *J. Am. Stat. Assoc.* **71**, 340 (1976).
- [53] S. A. Cushman, *Entropy* **20**, 314 (2018).